



**HAL**  
open science

# Passivity Analysis and Design of Passivity-Based Controllers for Trajectory Tracking at High Speed of Autonomous Vehicles

Gilles Tagne, Reine Talj, Ali Charara

► **To cite this version:**

Gilles Tagne, Reine Talj, Ali Charara. Passivity Analysis and Design of Passivity-Based Controllers for Trajectory Tracking at High Speed of Autonomous Vehicles. IEEE Intelligent Vehicles Symposium (IV 2014), Jun 2014, Dearborn, Michigan, United States. pp.1151-1156. hal-01061114

**HAL Id: hal-01061114**

**<https://hal.science/hal-01061114>**

Submitted on 5 Sep 2014

**HAL** is a multi-disciplinary open access archive for the deposit and dissemination of scientific research documents, whether they are published or not. The documents may come from teaching and research institutions in France or abroad, or from public or private research centers.

L'archive ouverte pluridisciplinaire **HAL**, est destinée au dépôt et à la diffusion de documents scientifiques de niveau recherche, publiés ou non, émanant des établissements d'enseignement et de recherche français ou étrangers, des laboratoires publics ou privés.

# Passivity Analysis and Design of Passivity-Based Controllers for Trajectory Tracking at High Speed of Autonomous Vehicles

Gilles Tagne, Reine Talj and Ali Charara

**Abstract**—Autonomous intelligent vehicles are under intensive development, especially this last decade. This paper focuses on the lateral control of intelligent vehicles, with the aim of minimizing the lateral displacement of the autonomous vehicle with respect to a given reference trajectory. The control input is the steering angle and the output is the lateral error displacement. After passivity analysis of the system to establish the properties of passivity between some inputs and outputs, we present design and validation of lateral controllers based on passivity, to ensure robust stability and good performances with respect to parametric variations and uncertainties encountered in driving applications. The control strategies have been validated in closed-loop on SCANer<sup>TM</sup> studio [1], a driving simulation engine, according to several real driving scenarios. The validation shows robustness and good performances of the proposed control approaches, and puts in evidence the improvement brought by the proposed Nested Passivity-Based Controller (PBC).

## I. INTRODUCTION

Several competitions have been organized all around the world to favor the development of autonomous intelligent vehicles, as the DARPA (Defense Advanced Research Projects Agency) Challenges at 2004, 2005 and 2007 in USA; the Korean Autonomous Vehicle Competitions (AVC) at 2010, 2012 and 2013, and many others. The introduction of autonomous vehicles could produce several advantages, mainly decreased road accidents. Indeed, the autonomous system is more reliable and faster to react than human drivers. Note that driver errors contribute wholly or partly to about 90% of crashes. Therefore, several research laboratories and companies are increasingly interested by the development of autonomous driving applications. See [2], [3] for some examples. This is an area of growing research and one of the major challenges today is to ensure autonomous driving at high speed.

Three main steps are necessary to ensure an autonomous navigation: the perception and localization, the path planning and the vehicle control. The vehicle control can be divided into two tasks: longitudinal control and lateral control. This paper focuses on the lateral control of intelligent vehicles. This is a very active research field that has been studied since the 1950s.

This work was carried out in the framework of the Labex MS2T, which was funded by the French Government, through the program Investments for the future managed by the National Agency for Research (Reference ANR-11-IDEX-0004-02).

The authors are working at Heudiasyc Laboratory, UMR CNRS 7253, Université de Technologie de Compiègne, BP 20529, 60205 Compiègne, France  
gilles.tagne@hds.utc.fr, reine.talj@hds.utc.fr,  
ali.charara@hds.utc.fr

Lateral control consists on handling the vehicle using the steering wheel to follow the reference trajectory. Given the high nonlinearity of the vehicle on one hand, and the uncertainties and disturbances in automotive applications on the other hand, a very important issue to be considered in the control design is the robustness. The controller should be able to reject the disturbances and deal with parameter uncertainties and variations.

In recent years, considerable research has been made to provide lateral guidance of autonomous vehicles. In literature, many control strategies have been developed. Simple PID controllers have been proposed in [4] and [5]. Moreover, other classical techniques have been used. We can cite  $H_\infty$  [6], state feedback [7], Lyapunov stability based control [8], fuzzy logic [9], linear quadratic optimal predictive control [10] and many others. On the other hand, Model Predictive Control (MPC) appears to be well suited to the trajectory following [11], [12]. In [13], Sliding Mode Control (SMC) has been applied. This control strategy is known for its robustness against uncertainties and its capacity to reject disturbances. However, its main drawback is the chattering.

In the literature, one can find also some comparisons between existing controllers. In [14], a comparison is made between proportional, adaptive,  $H_\infty$  and fuzzy controllers. More recently, in [15], a comparison of two controllers for trajectory tracking was performed. In [16], continuous-time and discrete-time switched  $H_\infty$  are compared. It is difficult to make an objective classification from the literature, but it is clear that different results showed that the class of adaptive controllers represents a very promising technique for such uncertain and nonlinear application.

For the best of our knowledge, and after a large bibliographical study, the characteristics of the vehicle dynamics have never been studied in means of energetic and passivity properties. However, if such properties exist, it could allow a very well comprehension of the system and of its inner interconnections. Such result could be the cornerstone for the development of a very promising family of passivity-based controllers, well suited for this uncertain and complex nonlinear system.

Passivity is a concept that represent a very interesting stability property of some physical systems. In fact, passive systems are a class of dynamical systems in which the energy exchange plays a central role. A passive system cannot store more energy than is supplied to it, what reflects a strong stability criterion. Theory of passivity is a framework for analyzing physical systems and designing controllers using a description of the input-output relationship based on

energy considerations. We study the passivity to analyze the frequency behavior, determine the passive outputs to easily control the system. We can therefore find the passivity as a way to impose robust stability by developing passivity-based controllers. This is particularly relevant in this application given the parametric variations and uncertainties (speed, curvature, road friction coefficient, etc...). In this paper, the passivity of several input-output maps of the system have been proved. Then, we present the design of two control laws based on the state feedback Passivity-Based Control (PBC). The first one is a simple PD and the second one is a Nested PBC.

To design the controllers, we consider that the vehicle is equipped with sensors and/or observers to measure yaw rate, lateral error and its derivative. To validate the control strategies, the closed-loop system with SCANer<sup>TM</sup> studio [1], a driving simulation engine, has been simulated according to several real driving scenarios. The validation shows robustness and good performances of the proposed control approaches.

This paper is organized as follows. Section II presents the dynamical models of the vehicle, used for control design and validation. In Section III, the control problem definition is presented, then the passivity analysis is presented in Section IV. The control strategies for lateral vehicle dynamics are developed in Section V. Section VI presents results. Finally, we conclude in Section VII, with some remarks and future work directions.

## II. DYNAMIC MODELS OF VEHICLE

To design the controller, a simple and widely used dynamic bicycle model [7] is considered. Dynamic equations in terms of slip angle and yaw rate of the bicycle model are given by:

$$\begin{aligned}\dot{\beta} &= -\frac{\mu(C_f+C_r)}{mV_x}\beta - \left(1 + \frac{\mu(L_f C_f - L_r C_r)}{mV_x^2}\right)\dot{\psi} + \frac{\mu C_f}{mV_x}\delta \\ \dot{\psi} &= -\frac{\mu(L_f C_f - L_r C_r)}{I_z}\beta - \frac{\mu(L_f^2 C_f + L_r^2 C_r)}{I_z V_x}\dot{\psi} + \frac{\mu L_f C_f}{I_z}\delta\end{aligned}\quad (1)$$

where  $\beta$ ,  $\psi$  and  $\delta$  represent respectively the sideslip angle, the yaw angle of the vehicle and the steering wheel angle (control input). Table I presents vehicle parameters and nomenclature.

TABLE I  
VEHICLE PARAMETERS AND NOMENCLATURE (BICYCLE MODEL)

$V_x$	Longitudinal velocity	-	[m/s]
$\beta$	Sideslip angle	-	[rad]
$\dot{\psi}$	Yaw rate	-	[rad/s]
$\delta$	Steering wheel angle	-	[rad]
$\mu$	Road friction coefficient	1	-
$m$	Mass	1719	[kg]
$I_z$	Yaw moment of inertia	3300	[kgm <sup>2</sup> ]
$L_f$	Front axle-COG distance	1.195	[m]
$L_r$	Rear axle-COG distance	1.513	[m]
$C_f$	Cornering stiffness of the front tire	170550	[N/rad]
$C_r$	Cornering stiffness of the rear tire	137844	[N/rad]

The proposed controllers have been validated in simulation in closed-loop with the car simulator SCANer<sup>TM</sup> studio [1]. This simulator use the vehicle full model (a more representative model) to represent the vehicle dynamics.

## III. CONTROL PROBLEM DEFINITION

The aim of the lateral control is to minimize the lateral displacement of the vehicle with respect to a given reference path. The lateral error dynamics at the center of gravity of the vehicle, with respect to a reference path, is given by  $\ddot{e} = a_y - a_{yref}$ ; where  $a_y$  and  $a_{yref}$  represent respectively the lateral acceleration of the vehicle, and the desired one on the reference path. Assuming that the desired lateral acceleration can be written as  $a_{yref} = V_x^2 \rho$ , where  $\rho$  is the curvature of the road, and given that  $a_y = V_x(\dot{\beta} + \dot{\psi})$  [7], we have:

$$\ddot{e} = V_x(\dot{\beta} + \dot{\psi}) - V_x^2 \rho \quad (2)$$

Replacing  $\dot{\beta}$  by its expression in equation (1), we obtain:

$$\ddot{e} = -\frac{\mu(C_f+C_r)}{m}\dot{\beta} - \frac{\mu(L_f C_f - L_r C_r)}{mV_x}\dot{\psi} - V_x^2 \rho + \frac{\mu C_f}{m}\delta \quad (3)$$

The new system state variables are  $x = (\beta, \psi, \dot{e}, e)^\top$  and has the following dynamics:

$$\dot{x} = Ax + B_1 \delta + B_2 \rho \quad (4)$$

where,

$$A = \begin{bmatrix} -\frac{\mu(C_f+C_r)}{mV_x} & -1 - \frac{\mu(L_f C_f - L_r C_r)}{mV_x^2} & 0 & 0 \\ -\frac{\mu(L_f C_f - L_r C_r)}{I_z} & -\frac{\mu(L_f^2 C_f + L_r^2 C_r)}{I_z V_x} & 0 & 0 \\ -\frac{\mu(C_f+C_r)}{m} & -\frac{\mu(L_f C_f - L_r C_r)}{mV_x} & 0 & 0 \\ 0 & 0 & 1 & 0 \end{bmatrix} \quad (5)$$

$$B_1 = \begin{bmatrix} \frac{\mu C_f}{mV_x} \\ \frac{\mu L_f C_f}{I_z} \\ \frac{\mu C_f}{m} \\ 0 \end{bmatrix}, \quad B_2 = \begin{bmatrix} 0 \\ 0 \\ -V_x^2 \\ 0 \end{bmatrix}$$

The control input is the steering wheel angle and the lateral error is the output. The aim of the lateral control is to cancel error of the lateral displacement. Then, for a given curvature  $\rho$  and longitudinal velocity  $V_x$ , the desired behavior corresponds to  $\dot{e} = e = 0$ . Hence, it is easy to prove that the desired equilibrium point is:

$$(\beta^*, \psi^*, \dot{e}, e)^\top = (\beta^*, \psi^*, 0, 0)^\top$$

with

$$\begin{aligned}\beta^* &= (L_r - \frac{L_f m V_x^2}{\mu C_r (L_f + L_r)})\rho \\ \psi^* &= V_x \rho\end{aligned}\quad (6)$$

At the equilibrium point, the control input is:

$$\delta^* = (L_f + L_r)\rho + \frac{mV_x^2(L_r C_r - L_f C_f)}{\mu C_f C_r (L_f + L_r)}\rho \quad (7)$$

Hence, define the new error variables:

$$\begin{cases} \tilde{\beta} = \beta - \beta^* \\ \tilde{\psi} = \psi - \psi^* \\ \tilde{\delta} = \delta - \delta^* \end{cases} \quad (8)$$

The error dynamics of the system (4) having the origin as equilibrium point  $(\tilde{\beta}, \tilde{\psi}, \dot{e}, e)^\top = (0, 0, 0, 0)^\top$  becomes:

$$\dot{\tilde{x}} = A\tilde{x} + B_1 \tilde{\delta} \quad (9)$$

where,  $A$  and  $B_1$  have been defined above (5).

#### IV. PASSIVITY ANALYSIS

The Kalman-Yakubovich-Popov (KYP) lemma is considered to be one of the pillars for control and systems theory. To demonstrate the passivity of an output, this lemma is considered [17].

**Proposition 1: The map  $\tilde{\delta} \rightarrow \ddot{e}$  is Strongly Strictly Passive.**

*Proof:* The proof of strong strict passivity is established showing that the transfer function  $H_0(s)$  of the map  $\tilde{\delta} \rightarrow \ddot{e}$  is Strongly Strictly Positive Real (SSPR).

Assume that the road coefficient of friction  $\mu = 1$ . Combining dynamic equations of the bicycle model in terms of slip angle and yaw rate (1) with the equation of lateral error dynamic (3), and after some calculations, one can find that the transfer function  $H_0(s)$  between  $\tilde{\delta}$  as input and  $\ddot{e}$  as output is given by:

$$H_0(s) = \frac{\ddot{e}(s)}{\tilde{\delta}(s)} = \frac{as^2 + bs + c}{s^2 + ds + f} \quad (10)$$

where,

$$\begin{cases} a = \frac{C_f}{m} \\ b = \frac{L_r C_f C_r (L_f + L_r)}{m L_z V_x} \\ c = \frac{C_f C_r (L_f + L_r)}{m L_z} \\ d = \frac{(C_f + C_r)}{m V_x} + \frac{(L_f^2 C_f + L_r^2 C_r)}{L_z V_x} \\ f = \frac{C_f C_r (L_f + L_r)^2}{m L_z V_x^2} + \frac{(L_r C_r - L_f C_f)}{L_z} \end{cases} \quad (11)$$

The transfer function  $H_0(s)$  has a relative degree equal to 0. Then, according to the KYP Lemma applied in the frequency domain, the proof of SSPR is tantamount to verifying :

$$\Re[H_0(j\omega)] \geq \zeta > 0, \forall \omega \in (-\infty, +\infty), \quad (12)$$

with  $\Re(\cdot)$ , the operator returning the real part.

Whatever the uncertainties and variations encountered, the model parameters ( $C_f, C_r, L_f, L_r, m, L_z$ ) are always positive. Thus, the coefficients  $a, b, c, d, f$  of  $H_0(s)$  are always positive. According to the criterion of Routh-Hurwitz, zeros and poles of  $H_0(s)$  are strictly stable, so  $H_0(s)$  is minimum phase and Hurwitz. Setting  $s = j\omega$ , one can prove that:

$$\Re[H_0(j\omega)] \geq \zeta > 0, \forall \omega \in (-\infty, +\infty) \quad (13)$$

hence, the transfer function  $H_0(s)$  is Strongly Strictly Positive Real (SSPR), yielding to the desired result. ■

**Proposition 2: The map output  $\tilde{\delta} \rightarrow \dot{e}$  is passive.**

*Proof:* The transfer function  $H_1(s)$  of the output  $\dot{e}$  with respect to the input  $\tilde{\delta}$  is given by:

$$H_1(s) = \frac{1}{s} H_0(s) \quad (14)$$

The transfer function  $H_1(s)$  is a cascade connection of an integrator with the strongly strictly positive real transfer function  $H_0(s)$ . Hence,  $H_1(s)$  is positive real, yielding the passivity of the map  $\tilde{\delta} \rightarrow \dot{e}$ , the desired result. For more details see [17]. ■

**Proposition 3: The map  $\tilde{\delta} \rightarrow \dot{\psi}$  is Strictly Passive.**

*Proof:* The proof is established at the same manner of the previous subsections. ■

**Proposition 4: The map  $\tilde{\delta} \rightarrow \tilde{\beta}$  is not passive.**

*Proof:* The transfer function  $H_3(s)$  of  $\tilde{\beta}$ , relative to the input  $\tilde{\delta}$  is given by:

$$H_3(s) = \frac{\tilde{\beta}(s)}{\tilde{\delta}(s)} = \frac{ks + l}{s^2 + ds + f} \quad (15)$$

where,

$$\begin{cases} d \text{ and } f \text{ defined in (11),} \\ k = \frac{C_f}{m V_x} \\ l = \frac{L_r C_f C_r (L_f + L_r)}{m L_z V_x^2} - \frac{L_f C_f}{L_z} \end{cases}$$

The transfer function  $H_3(s)$  has a relative degree equal to 1. The variables  $d, f$  and  $k$  are always positive, but  $l$  can be either positive or negative depending on the value of  $V_x$  and other parameters. When  $l < 0$ ,  $H_3(s)$  has a negative zero, and is not positive real, what proves the proposition. ■

The zero of the transfer function  $H_3(s)$  is stable if and only if  $l$  is positive, i.e.

$$-\frac{L_f C_f}{L_z} + \frac{L_r C_f C_r (L_f + L_r)}{m L_z V_x^2} > 0,$$

hence,

$$V_x < \sqrt{\frac{L_r C_r (L_f + L_r)}{L_f m}}. \quad (16)$$

This fact can be understood as if the map  $\tilde{\delta} \rightarrow \tilde{\beta}$  is passive when the speed is limited as in (16), and this characteristic is stolen at high speeds. Using the parameters given in Table I, the speed limit of equation (16) corresponds to  $V_x < 16.5 \text{ m/s} \simeq 60 \text{ km/h}$ .

**Proposition 5: The map  $\dot{\psi} \rightarrow \ddot{e}$  is Strictly Passive and the map  $\dot{\psi} \rightarrow \dot{e}$  is Passive.**

*Proof:* The proof is established at the same manner of the previous subsections. ■

Summarizing, considering the error system (9) with the control input  $\tilde{\delta}$ , then the output  $\dot{e}$  is passive (P). This is an interesting property of the system that favor the design of passivity based controllers (PBC) using a feedback on this passive output.

On the other hand, the map  $\tilde{\delta} \rightarrow \dot{\psi}$  is strictly passive (SP); moreover, the map  $\dot{\psi} \rightarrow \dot{e}$  is passive. The passivity of these two cascaded subsystems could be interesting to develop nested (PBC) with the intermediate variable  $\dot{\psi}$ . The Fig. 1 can resume the passivity maps of the system.

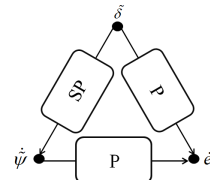


Fig. 1. Passivity maps of the system

## V. PBC CONTROLLERS DESIGN

Consider the diagram of Fig. 2, where  $S_1$  is the system and  $S_2$  the controller. Two reasonings can be used to analyze the stability of the closed-loop system. We can seek an energy function based on the closed-loop system. This can typically be obtained by a Lyapunov function. Or we can try to interpret this as a negative dynamic interconnection of two blocks. Specifically, for systems with structural characteristics of passivity, we can try to interpret this as a negative dynamic interconnection of two passive systems then use the passivity theorem [18] to conclude on the stability of the closed-loop system. Obviously, as the system has characteristics of passivity, we will use the second reasoning (equivalent closed-loop interconnections), which is more intuitive. The following corollary (corollary 4.1 in [17]) remind a very useful property of stability of two systems on feedback interconnections.

*Corollary 1:* Considering the diagram of Fig. 2, this feedback system with finite gains is stable if either of the following statements is true:

- $S_1$  is Passive (P) and  $S_2$  is Input Strictly Passive (ISP).
- $S_1$  is Output Strictly Passive (OSP) and  $S_2$  is Passive.

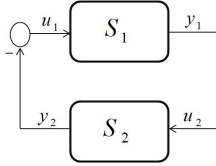


Fig. 2. Feedback interconnection of passive systems scheme

### A. PD controllers

The aim of the lateral control of autonomous intelligent vehicles is to minimize the lateral displacement of the vehicle with respect to a given reference path. Consider the system (9) in which  $\tilde{\delta}$  is the input and lateral error  $e$  is the output. The PD controller applied to that system is given by the following input:

$$\tilde{\delta} = -K_D \dot{e} - K_P e \quad (17)$$

where  $K_D$  and  $K_P$  are state-feedback positive gains.

It is important to note that a PD with the output  $e$  is equivalent to a PI with the passive output  $\dot{e}$ . So, we can interpret the closed-loop system as the interconnection of two subsystems with respectively inputs  $u_1$  and  $u_2$  and outputs  $y_1$  and  $y_2$  as:

$$\begin{cases} y_1 = u_2 = \dot{e} \\ u_1 = -y_2 = \tilde{\delta} \end{cases} \quad (18)$$

We have  $S_1 = H_1$  is passive (see Section IV, Proposition 2).

$$S_2(s) = \frac{K_P + K_D s}{s}$$

$S_2$  defines an Input Strictly Passive (ISP); It is easy to show that:

$$\Re [S_2(j\omega)] \geq \varepsilon > 0, \forall \omega \in (-\infty, +\infty)$$

So the closed-loop system is stable and describes a passive map between the input and the output.

Stability of the system is assured with the PD controller for all gains  $K_D$  and  $K_P$  positive. This has also been shown in [7]. Note that the gains are chosen taking into account practical considerations and the desired performances. Finally, the control input applied to the system (4) is:

$$\delta_{PD} = \tilde{\delta} + \delta^* = -K_P e - K_D \dot{e} + (L_f + L_r) \rho + \frac{mV_x^2(L_r C_r - L_f C_f)}{\mu C_f C_r (L_f + L_r)} \rho \quad (19)$$

With this classical PD controller, we have robust stability unfortunately the performance depends on parameters of the system. To have good performance over a wide operating range, such a controller must be adaptive gains. In [19], the proposed controller by Immersion and Invariance (I&I) can be interpreted as a dynamic state feedback and an adaptive PD, where the gains depend on the parameters. This control law is given by:

$$\tilde{\delta}_{I\&I} = -\frac{mK\lambda}{C_f} e - \frac{m(K+\lambda)}{C_f} \dot{e} + \frac{C_f + C_r}{C_f} \tilde{\beta} + \frac{L_f C_f - L_r C_r}{C_f V_x} \dot{\psi} \quad (20)$$

With this command, performance can be fixed in advance. Its main drawback is that, large parametric uncertainties degrade performances.

With controllers that have a PD structure, one gets a robust stability. With PI structure, robustness against uncertainties and disturbances can be improved, but the system becomes easily destabilizable. In the next paragraph, we will develop a nested controller based on the passivity properties of the system, to obtain a good compromise between robust stability, and robustness against parametric uncertainties and disturbances. Indeed, the closed-loop system preserves its passivity properties necessary for high speed driving while having good performance.

### B. Nested Passive Controllers (Nested PBC)

Considering the Fig. 1 and knowing that the yaw rate dynamics is faster than the lateral error dynamics, we can decompose the lateral controller into two passive nested controllers. This is a major interest since  $e$  and  $\dot{\psi}$  are controlled simultaneously. We can therefore create two separate controllers for each own dynamics based on its characteristic of passivity. In this subsection, we develop a control strategy of an autonomous vehicle using two passive controllers to ensure guidance and stability in two separate loops. The outer controller minimizes the lateral error. The inner controller minimizes the yaw rate error by providing the corresponding steering angle. The particularity of such a strategy is double: it helps designing a robust controller while preserving the passivity properties of the closed-loop system to ensure good performance. If necessary, two controllers of different natures can be used, in order to benefit from the robustness of each. It also allows an control of the lateral error and the yaw rate error. Fig. 3 scheme illustrates the proposed control strategy.

*Proposition 6:* Considering the diagram in Fig. 3 (where the control is achieved respectively by two PD and PI controllers), the closed-loop system is stable and passive.

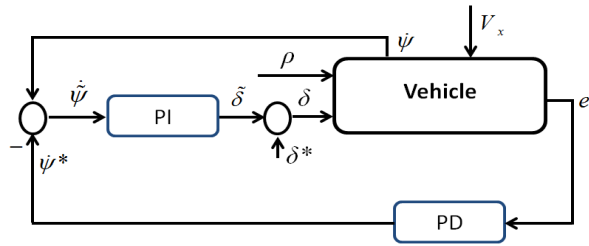


Fig. 3. Nested PBC control strategy

*Proof:* The proof is relatively simple, corollary 1 allows to show it. ■

### Synthesis of the outer controller:

This controller is designed to cancel the lateral error  $e$ . The control input is the yaw rate error.

Subsystem  $\Sigma_1 : \dot{\psi} \mapsto \dot{e}$  is passive (P), so any ISP controller guarantee stability and passivity of the closed-loop system. In this paper, we choose a simple PI. We remind that a PI applied to the passive output  $\dot{e}$  is equivalent to a PD applied to the output  $e$ . So, the outer control input of the controller is given by:

$$\dot{\psi} = -K_{D1}\dot{e} - K_{P1}e \quad (21)$$

where  $K_{D1}$  and  $K_{P1}$  are positive gains.

### Synthesis of the inner controller:

This controller is designed to cancel the yaw rate error with respect to the reference given by the outer controller. The control input is the steering angle  $\delta$ .

Subsystem  $\Sigma_2 : \delta \mapsto \dot{\psi}$  is strictly passive (SP), so any passive (P) controller guarantee stability and passivity of the closed-loop system. In this paper, we choose a PI. The control input of the inner controller is given by:

$$\dot{\delta} = -K_{I2} \int \dot{\psi} - K_{P2} \dot{\psi} \quad (22)$$

where  $K_{I2}$  and  $K_{P2}$  are positive gains.

Given the strict passivity (SP) of the output  $\dot{\psi}$  for an input  $\dot{\delta}$ , the closed-loop system with a PI controller is stable and passive. Note that any passive controller, a simple proportional for example, would achieve the same result. The addition of integral action, well known to reject constant disturbances also has the advantage that the controller can be implemented without the knowledge of  $\delta^*$  which depends on the uncertain model parameters.

## VI. SIMULATION RESULTS

To validate our control laws, tests have been performed on the simulation environment SCANeR<sup>TM</sup> studio, a driving simulation engine, according to several real driving scenarios. For control laws, we used the following values of the gains:  $K_P = 0.08$  and  $K_D = 0.01$  for the PD controller.  $K_{P1} = 10$ ,  $K_{D1} = 1$ ,  $K_{P2} = 0.05$  and  $K_{I2} = 0.02$  for the Nested PBC, with the nominal vehicle parameters (see Table I). To highlight the improvements brought by the PBC controllers, a comparison with a previously developed I&I controller [19] was made. The tests are performed on a road with a curvature varying between  $-0.02$  and  $+0.02m^{-1}$  (see Fig. 4).

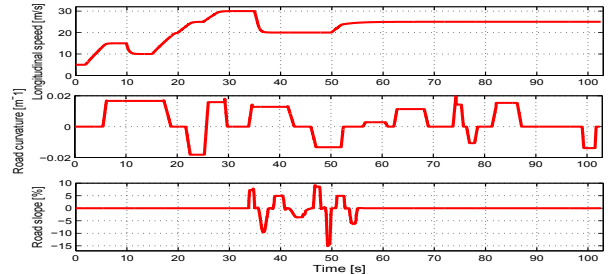


Fig. 4. Road informations and longitudinal speed

### A. Test of the controllers with nominal parameters

This test was made with the goal of verifying the capacity of controllers to track the reference trajectory during normal driving with known nominal parameters. Fig. 5 presents different curves: the reference path and the trajectories followed by the controlled vehicles; the lateral error and the yaw angle error. All controllers ensure the reference tracking with low errors (the lateral displacement of the closed-loop system remains smaller than 15cm in this test conditions). Note that the PD controller is less robust to curvature variations. This controller requires only the measurement of the lateral error, what is not sufficient to ensure a robust tracking in highly nonlinear areas. For small changes in curvature, the errors of the three controllers are almost similar.

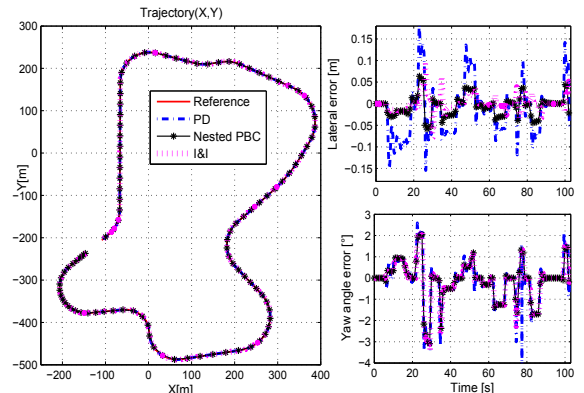


Fig. 5. Trajectories; reference and control laws

This test shows the good performance of I&I and Nested PBC controllers during normal driving at high and varying speed, and varying curvature, when the nominal parameters are known. We will evaluate the robustness of these two controllers with respect to parametric uncertainties.

### B. Robustness to vehicle parameter uncertainties

In this subsection, we evaluate the robustness of the controllers with respect to parametric uncertainties of the vehicle. It is important to note that the parametric uncertainties can be due to the fact that the parameters may vary, but are considered to be fixed for the command. This is the case of the mass of the vehicle, for example.

Fig. 6 presents lateral errors for uncertainties on the value of the cornering stiffness for previous test. Fig. 7 presents the robustness of the control laws against the uncertainties on the vehicle mass. For uncertainties in the order of  $+/-15\%$ , on the value of cornering stiffness (or of  $+/-10\%$  for mass), PBC controllers are able to follow the path with almost

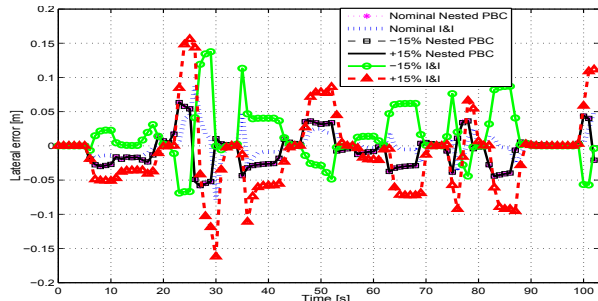


Fig. 6. Robustness against uncertainties of cornering stiffness

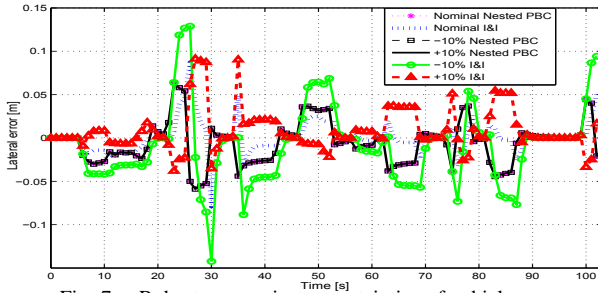


Fig. 7. Robustness against uncertainties of vehicle mass

similar errors. The errors of the *I&I* remain acceptable (we consider that the maximum error should not be greater than  $\pm 20\text{cm}$  to ensure safe driving).

With the *I&I* controller, the error depends strongly on the value of the parametric uncertainty. The passive controller (Nested PBC) is more robust to parameter uncertainties. Indeed, the inputs of the controller depend only on passive outputs (errors), which do not depend on uncertain parameters. However, the input of the *I&I* controller depends on these parameters. Moreover, the PBC controller also has the advantage of using less measurements than the previous one. Indeed, the *I&I* controller needs an estimation of the sideslip angle. Hence, these results put in evidence the improvement brought by the Nested PBC controller.

## VII. CONCLUSION

In this paper, after a detailed study of the passivity properties of the model, controllers based on these properties are proposed to ensure a robust trajectory following. The design of two controllers was presented: a simple PD controller and a nested PBC controller. They guarantee robust stability (not depending on the value of the system parameters) and passivity of the closed-loop system. Results show that a greater consideration of structural features of the model during the design of a controller—namely the passivity properties—can significantly improve the robustness of the controller for autonomous driving applications. To illustrate this improvement, a comparison was made with an Immersion and Invariance controller developed previously in [19]. The validation shows robustness and good performance of the proposed Nested PBC controller.

In this paper, the study of passivity properties has been done considering the road coefficient of friction  $\mu = 1$ . An analysis for variant  $\mu$  will be studied by the authors. In addition, a study of robustness based on sensitivity analysis will be performed. Moreover, an adaptive version of the Nested PBC controller is under study.

## REFERENCES

- [1] "<http://www.sera-cd.com>, <http://www.scanersimulation.com>."
- [2] J. Wei, J. M. Snider, J. Kim, J. M. Dolan, R. Rajkumar, and B. Litkouhi, "Towards a viable autonomous driving research platform," in *Int. IEEE Conference on Intelligent Vehicles Symposium (IV)*, pp. 763–770, 2013.
- [3] M. Bertozzi, L. Bombini, A. Broggi, M. Buzzoni, E. Cardarelli, S. Cattani, P. Cerri, A. Coati, S. Debatisti, A. Falzoni, R. I. Fedriga, M. Felisa, L. Gatti, A. Giacomazzo, P. Grisleri, M. C. Laghi, L. Mazzei, P. Medici, M. Panciroli, P. P. Porta, P. Zani, and P. Versari, "VIAC: An out of ordinary experiment," in *Int. IEEE Conference on Intelligent Vehicles Symposium (IV)*, (Baden- Baden), pp. 175–180, 2011.
- [4] A. Broggi, M. Bertozzi, and A. Fascioli, "The ARGO autonomous vehicle's vision and control systems," *Int. Journal of Intelligent Control and Systems*, vol. 3, no. 4, pp. 409–441, 1999.
- [5] P. Zhao, J. Chen, T. Mei, and H. Liang, "Dynamic motion planning for autonomous vehicle in unknown environments," in *Int. IEEE Conference on Intelligent Vehicles Symposium (IV)*, 2011.
- [6] S. Hima, B. Lusseti, B. Vanholme, S. Glaser, and S. Mammari, "Trajectory Tracking for Highly Automated Passenger Vehicles," in *International Federation of Automatic Control (IFAC) World Congress*, (Milano), pp. 12958–12963, 2011.
- [7] R. Rajamani, *Vehicle dynamics and control*. Springer, 2006.
- [8] A. Benigne-Neto, S. Scalzi, S. Mammari, and M. Netto, "Dynamic controller for lane keeping and obstacle avoidance assistance system," in *Int. IEEE Conference on Intelligent Vehicles Symposium (IV)*, pp. 1363–1368, 2010.
- [9] J. Naranjo, C. Gonzalez, R. Garcia, and T. de Pedro, "Lane-Change Fuzzy Control in Autonomous Vehicles for the Overtaking Maneuver," *Int. IEEE Transactions on Intelligent Transportation Systems*, vol. 9, pp. 438–450, Sept. 2008.
- [10] D. Kim, J. Kang, and K. Yi, "Control strategy for high-speed autonomous driving in structured road," in *Int. IEEE Conference on Intelligent Transportation Systems (ITSC)*, 2011.
- [11] J. Levinson, J. Askeland, J. Becker, J. Dolson, D. Held, S. Kammel, J. Z. Kolter, D. Langer, O. Pink, V. Pratt, M. Sokolsky, G. Stanek, D. Stavens, A. Teichman, M. Werling, and S. Thrun, "Towards Fully Autonomous Driving : Systems and Algorithms," in *Int. IEEE Conference on Intelligent Vehicles Symposium (IV)*, (Baden-Baden), pp. 163–168, 2011.
- [12] T. Besselmann and M. Morari, "Autonomous Vehicle Steering Using Explicit LPV-MPC," in *European Control Conference (ECC)*, (Budapest), pp. 2628–2633, 2009.
- [13] G. Tagne, R. Talj, and A. Charara, "Higher-Order Sliding Mode Control for Lateral Dynamics of Autonomous Vehicles , with Experimental Validation," in *Int. IEEE Conference on Intelligent Vehicles Symposium (IV)*, (Gold Coast), pp. 678–683, 2013.
- [14] S. Chaib, M. Netto, and S. Mammari, "H inf, adaptive, PID and fuzzy control: a comparison of controllers for vehicle lane keeping," in *Int. IEEE Intelligent Vehicles Symposium (IV)*, pp. 139–144, 2004.
- [15] D. Heß, M. Althoff, and T. Sattel, "Comparison of Trajectory Tracking Controllers for Emergency Situations," in *Int. IEEE Conference on Intelligent Vehicles Symposium (IV)*, (Gold Coast), pp. 163–170, 2013.
- [16] L. Menhour, D. Koenig, and B. Andr, "Continuous-Time and Discrete-Time Switched H inf. State Feedback Controllers : Application for a Robust Steering Vehicle Control," in *European Control Conference (ECC)*, (Zurich), pp. 986–991, 2013.
- [17] R. Lozano, B. Brogliato, O. Egeland, and B. Maschke, *Dissipative Systems Analysis and Control: Theory and Applications*. Springer, 2000.
- [18] D. Hill and P. Moylan, "The stability of nonlinear dissipative systems," *IEEE Transactions on Automatic Control*, vol. 21, no. 5, pp. 708–711, 1976.
- [19] G. Tagne, R. Talj, and A. Charara, "Immersion and Invariance Control for Reference Trajectory Tracking of Autonomous Vehicles," in *Int. IEEE Conference on Intelligent Transportation Systems (ITSC)*, (The Hague), pp. 2322–2328, 2013.